Frontiers in Bioscience Landmark

Front. Biosci. (Landmark Ed) **2026**; 31(5): 51227
https://doi.org/10.31083/FBL51227

Original Research

miR-19a-3p as a Candidate oncomiRNA in Cervical Cancer: Insights From a Bioinformatic Analysis

Ramón Antaño-Arias[1], Francisco Israel Torres-Rojas[1], Gabriela Elizabeth Campos-Viguri[2], Adán Arizmendi-Izazaga[3], Julio Ortiz-Ortiz[3,4], Roberto Dircio-Maldonado[5], Judit Alarcón-Millán[4,5,6], Fredy David Bartolo-Ángel[3,4,5], Alejandro Fiallo-Rodríguez[3,4,5], Hilda Jiménez-Wences[3,4,5,*], Eric Genaro Salmerón-Bárcenas[7,*]

[1]Laboratory of Molecular Biomedicine, Faculty of chemical and Biological Sciences, Autonomous University of Guerrero, 39090 Chilpancingo, Guerrero, Mexico
[2]Center for Research in Applied Science and Advanced Technology, Morelos Unit, National Polytechnic Institute, 62790 Atlacholoaya, Morelos, Mexico
[3]Laboratory of Research in Metabolism and Cancer, Faculty of Chemical-Biological Sciences, Autonomous University of Guerrero, 39090 Chilpancingo, Guerrero, Mexico
[4]Laboratory of Research in Biomolecules, Faculty of Chemical-Biological Sciences, Autonomous University of Guerrero, 39090 Chilpancingo, Guerrero, Mexico
[5]Laboratory of Research in Infectious Diseases and Cancer, Faculty of Chemical-Biological Sciences, Autonomous University of Guerrero, 39090 Chilpancingo, Guerrero, Mexico
[6]Bacteriology Research Laboratory, Faculty of Chemical-Biological Sciences, Autonomous University of Guerrero, 39090 Chilpancingo, Guerrero, Mexico
[7]Department of Molecular Biomedicine, Center for Research and Advanced Studies, 07360 Mexico City, Mexico
*Correspondence: hjimenez@uagro.mx (Hilda Jiménez-Wences); eric.salmeron@cinvestav.mx (Eric Genaro Salmerón-Bárcenas)
Academic Editors: Giovanni Tossetta and Chen Li
Submitted: 25 February 2026 Revised: 15 April 2026 Accepted: 30 April 2026 Published: 21 May 2026

Abstract

Background: Cervical cancer (CC) remains a significant threat to global public health, with high incidence and mortality rates. Understanding the molecular mechanisms governing CC progression is critical for developing novel diagnostic and therapeutic strategies. microRNAs (miRNAs) have emerged as important regulators in cancer biology. This study aimed to identify and characterize a miRNA involved in CC development to assess and its potential as a diagnostic and prognostic biomarker through integrative bioinformatic and experimental analyses. **Methods**: Differentially expressed miRNAs (DEmiRNAs) were identified in CC using microarrays, after which *miR-19a-3p* expression trends were validated in multiple publicly available datasets. *miR-19a-3p* target genes were identified using the miRNAs Data Base (miRDB) and TargetScan databases. Pathway and biological process analyses were conducted with the Enrichr database. Target prediction and correlation analyses were used to explore potential interactions between *miR-19a-3p* and brain derived neurotrophic factor-antisense (*BDNF-AS*). Survival and diagnostic value were evaluated using Kaplan-Meier and receiver operating characteristic (ROC) curves. **Results**: In total, 24 DEmiRNAs were identified in CC, and *miR-19a-3p* expression patterns were validated in two independent datasets. This miRNA was predicted to regulate genes involved in transcription. The long non-coding RNA (lncRNA) *BDNF-AS* was identified as a potential target of *miR-19a-3p*. In ROC curve analyses, both *miR-19a-3p* and *BDNF-AS* showed potential diagnostic value. Functional enrichment implicated pathways involved in tumor progression. Low *BDNF-AS* expression was associated with poorer overall survival, consistent with prognostic potential. **Conclusions**: Together, the results of these bioinformatic analyses suggest that *miR-19a-3p* may act as an oncomiR in CC, potentially contributing to its pathogenesis through interactions with the *BDNF-AS* lncRNA.

Keywords: uterine cervical neoplasms; RNA, untranslated; *miR-19a-3p*; gene expression; *BDNF-AS*; biomarkers; bioinformatic analysis

1. Introduction

Cancer is a persistent public health problem, with an estimated 20.0 million new cases and 9.7 million cancer deaths worldwide in 2022. Cervical Cancer (CC) is the cancer with the 4th highest incidence (6.8%) and mortality (8.1%) among women globally. According to Global Cancer Observatory: CANCER TODAY (GLOBOCAN), an estimated 661,021 new CC cases and 348,189 CC-associated deaths occurred in 2022. CC also ranks as the 2nd most common and deadliest cancer in countries with a low/medium Human Development Index [1]. Similarly, CC ranked 3rd in incidence and mortality among cancers of the female genital system in 2024 in the USA [2]. There is thus a pressing need to clarify the molecular biology of

CC to develop new diagnostic, prognostic, and therapeutic biomarkers suitable for combatting this deadly malignancy.

Infection by high-risk human papillomavirus (HR-HPV) strains, including *genotypes 16* and *18*, is necessary but not sufficient for CC development. *HR-HPV 16* and *18* promote CC development through their E6 and E7 oncoproteins [3]. In addition, several genetic and epigenetic factors associated with CC have been identified, including variants at the *human leukocyte antigen* (*HLA*) locus on chromosome 6p21.3 and the aberrant methylation of promoters upstream of tumor suppressor genes and non-coding RNAs (ncRNAs) [4,5].

In general, ncRNAs are a class of RNAs that are not translated into proteins, including lncRNAs, circular RNAs (circRNAs), heterogeneous nuclear RNAs, PIWI-interacting RNAs (piRNAs), ribosomal RNAs, small nuclear RNAs, small nucleolar RNAs, transfer RNAs, and microRNAs (miRNAs) [6]. miRNAs are small ncRNA molecules of ~22 nucleotides that bind to seed sequences in the 3′ untranslated region (UTR), 5′ UTR, or coding regions of target mRNAs, inhibiting gene expression at the post-transcriptional level [7]. Moreover, miRNAs can act as molecular sponges, also known as competing endogenous RNAs or ceRNAs, and deregulate the expression of other ncRNAs, such as lncRNAs and circRNAs, thereby affecting key cellular processes [8–10]. Through these mechanisms, miRNAs regulate biological processes, including cell differentiation, angiogenesis, migration, and apoptosis [11]. Alterations in the expression of miRNAs are a common molecular event in the biology of multiple diseases, including neurodevelopmental conditions, autoimmunity, and cancer [11,12]. Therefore, the aim of the present study was to identify potential oncomiRNAs and explore their roles in CC through a bioinformatics approach.

miR-19a-3p acts as a tumor suppressor miRNA in several human cancers, including myeloma [13]. In contrast, *miR-19a-3p* acts as an oncogenic miRNA in hepatocellular carcinoma [14,15] and lung adenocarcinoma [16]. Recently, this miRNA was reported to promote CC development by acting as a ceRNA, thereby downregulating the expression of the lncRNA RNA Binding Protein, MRNA Processing Factor-Antisense 1 (RBPMS-AS1). The direct interaction between *miR-19a-3p* and this lncRNA was validated through functional assays to explore its role in CC [17]. However, it remains possible that *miR-19a-3p* may promote CC development by downregulation other ncRNAs with tumor suppressor activity, underscoring the need to fully explore the target lncRNAs associated with this miRNA in the context of CC.

In this study, *miR-19a-3p* overexpression was detected in CC using the miR-TV and Gene Expression Omnibus (GEO) databases. The potential role of this miRNA in CC was then explored by identifying its potential target genes, as well as associated pathways and biological processes, with the miRDB, TargetScan, and Enrichr databases. Ensembl database analysis revealed three potential *miR-19a-3p* binding sites in the lncRNA *BDNF-AS*, and a negative correlation between *miR-19a-3p* and *BDNF-AS* in CC was noted in the ENCORI database, supporting the potential relevance of this lncRNA as a target of *miR-19a-3p*. We additionally analyzed *BDNF-AS* expression in CC with the OncoDB and GEO databases, confirming its downregulation in CC. Subsequent, Enrichr database pathway and biological process analysis of genes significantly correlated with *BDNF-AS* expression revealed pathways and biological processes regulated by this lncRNA in CC. Finally, Gene Set Enrichment Analysis (GSEA) was performed in patients with CC and high or low *BDNF-AS* expression.

2. Materials and Methods

2.1 Cell Culture

The SiHa (HTB-35), HeLa (CCL-2) and C-33A (HTB-31™) cell lines were purchased from American Type Culture Collection (ATCC, Manassas, VA, USA). SiHa and C-33A cells were cultured in high-glucose Dulbecco's Modified Eagle's Medium (DMEM) (11-965-092, Gibco™; Carlsbad, CA, USA). HeLa cells were cultured in a 1:1 mixture of DMEM/F12 medium (DMEM/F12) (Cat: DFP44, Caisson Labs, Inc, Smithfield, UT, USA). All culture media were supplemented with 10% fetal bovine serum (FBS) (Cat: A5256701, Gibco™, Grand Island, NE, USA), 100 U/mL penicillin, 100 µg/mL streptomycin and 0.25 µg/mL Amphotericin B. Cells were grown at 37 °C in a 5% CO_2 incubator. All cell lines were authenticated by STR profiling and tested negative for mycoplasma.

2.2 RNA Isolation

Total RNA was isolated using TRIzol (Cat: 15596026, Invitrogen, Waltham, MA, USA) according to the manufacturer's instructions. The concentration and purity of total RNA were determined with a NanoDrop™ 2000/2000c UV-Vis spectrophotometer (Thermo Fisher Scientific, Waltham, MA, USA) based on the A260/A280 ratio. The integrity of total RNA was evaluated through 1% agarose gel electrophoresis. Total RNA was treated with RNase-free DNase I (Cat: EN0521, Thermo Scientific, Waltham, MA, USA). Finally, DNase-treated RNA was re-quantified using the NanoDrop™ 2000/2000c UV-Vis spectrophotometer (Thermo Fisher Scientific, Waltham, MA, USA) based on the A260/A280 ratio, followed by storage at –80 °C prior to cDNA synthesis.

2.3 cDNA Synthesis

cDNA synthesis for *miR-19a-3p* was performed with the TaqMan® MicroRNA Reverse Transcription kit (Cat: 4366596, Applied Biosystems, Vilnius, Lithuania) according to the manufacturer's instructions. The reaction mixture contained 5 ng of total RNA, RT Primer Pool (10 µM), dNTPs with dTTP (10 µM), MultiScribe Reverse Transcriptase (50 U/µL), RT Buffer (10X), RNase Inhibitor

(20 U/µL) and Nuclease-free water. Thermocycler settings were as follows: 30 min at 16 °C, 30 min at 42 °C, and 5 min at 85 °C.

cDNA synthesis for *BDNF-AS* was conducted using SuperScript III reverse transcriptase (Cat: 18080-044, Thermo Fisher Scientific, Waltham, MA, USA) following the manufacturer's instructions.

cDNAs concentrations were quantified using the NanoDrop™ 2000/2000c UV-Vis spectrophotometer (Thermo Fisher Scientific, Waltham, MA, USA), followed by storage at –20 °C prior to downstream use.

2.4 Real-Time Quantitative PCR (RT-qPCR)

miR-19a-3p levels were quantified with the hsa-*miR-19a-3p* assay ID: 000395 (Cat: Assay ID: 000395, Applied Biosystems, Waltham, MA, USA) and the TaqMan microRNA assay kit (Cat: 4427975, Applied Biosystems, Waltham, MA, USA) using the ABI 7500 Real-Time PCR System (Applied Biosystems, Waltham, MA, USA). The reaction mixture contained 1 µL of cDNA, TaqMan™ Small RNA Assay (20×), PCR Master Mix (2×), and Nuclease-free water. The thermocycler settings were: 20 s at 95 °C, followed by 40 cycles of 95 °C for 3 s and 60 °C for 30 s.

BDNF-AS expression levels were analyzed by RT-qPCR in reactions containing 200 ng of cDNA, primers at a final concentration of 1 µM, Power SYBR® Green PCR Master Mix 2× (Cat: 4368577, Applied Biosystems, Waltham, MA, USA), and Nuclease-free water. Analyses were performed using a PCR CFX96TM Real-Time PCR Detection System (Bio-Rad, Foster City, CA, USA) with the following thermocycler settings: 10 min at 95 °C, followed by 40 cycles of 95 °C for 20 s, 60 °C for 20 s, and 72 °C for 50 s. Primers used in this study were *BDNF-AS* sense: 5′-CCGTGAGAAGATCTCATTGGG-3′ and *BDNF-AS* antisense: 5′-GGGTCACAAGTCACGTAGCA-3′; Glyceraldehyde-3-Phosphate Dehydrogenase (GAPDH) sense: 5′-CCAGGTGGTCTCCTCTGACTT-3′ and GAPDH antisense: 5′-GTTGCTGTAGCCAAATTCGTTGT-3′.

The relative expression of *miR-19a-3p* and *BDNF-AS* was determined using the $2^{-\Delta\Delta Ct}$ method [18] with the respective normalization to U6 and GAPDH as housekeeping controls. Two biological replicates were included in these analyses, each with two technical replicates. *miR-19a-3p* and *BDNF-AS* expression data were Log_2-transformed. Significance was assessed using Student's *t*-tests in GraphPad Prism v8.0.2 (GraphPad Software, La Jolla, CA, USA). A p-value < 0.05 was considered statistically significant.

2.5 Expression Analysis

DEmiRNAs were identified when comparing CC and normal tissue samples from the GSE86100 dataset [19] using the GEO2R software (https://www.ncbi.nlm.nih.gov/geo/geo2r/) [20]. This dataset was selected based on the following criteria: (1) all cervical specimens were confirmed as squamous cell carcinoma through pathological examination, (2) patients had not received any chemotherapy treatment, and (3) control samples were confirmed to be normal using cytologic tests. The GSE86100 dataset (Platform: GPL19730, Agilent - 046064 Unrestricted_Human_miRNA_V19.0_Microarray, Probe Name version) consists of 6 HR-HPV-positive CC tissue samples (named as CC samples) and 6 uninfected normal mucosa tissue samples (named as controls samples). The microarray platform version used for this dataset was in format 8 × 60, including probes corresponding to 2006 human miRNAs. DEmiRNAs were identified based on the following criteria when comparing 6 CC and 6 controls samples: Fold Change (FC) >2 and p-value < 0.001.

miR-19a-3p and *BDNF-AS* expression analyses were performed in CC and normal tissue samples from the Cancer Genome Atlas (TCGA) dataset using the miR-TV [21] and OncoDB [22] databases. Expression data were downloaded and transformed into the RPM Log_2 format. Significant differences were determined using Mann-Whitney U-tests, with p-value < 0.05 as the threshold for significance.

miR-19a-3p expression was additionally analyzed in the GSE30656 (https://www.ncbi.nlm.nih.gov/geo/query/acc.cgi?acc=GSE30656) [23] dataset, while *BDNF-AS* expression was analyzed in the GSE67522 (https://www.ncbi.nlm.nih.gov/geo/query/acc.cgi?acc=GSE67522) [24,25] and GSE63514 (https://www.ncbi.nlm.nih.gov/geo/query/acc.cgi?acc=GSE63514) [26] datasets from the GEO [20,27] database. The GSE30656 dataset (Platform: GPL6955, Agilent-016436 Human miRNA Microarray 1.0, Feature Number version) contains 19 cervical adenocarcinoma/squamous cell carcinoma tissue samples and 10 cervical squamous epithelial samples with normal histology. The GSE67522 dataset (Platform: GPL10558, Illumina HumanHT-12 V4.0 expression beadchip) includes 20 HPV16 positive CC tissue samples and 22 HPV negative histologically normal controls/HPV16-positive non-malignant tissue samples. The GSE63514 dataset (Platform: GPL570, [HG-U133_Plus_2] Affymetrix Human Genome U133 Plus 2.0 Array) contains 28 CC tissue samples and 24 normal tissue samples. Expression analysis was done with the GEO2R [20] software. Expression data were Log_2-transformed, and differences between groups were analyzed with Student's *t*-tests. A p-value < 0.05 was considered significant.

Differentially expressed genes (DEGs) between CC patient samples with high and low levels of *BDNF-AS* expression from the TCGA-CESC dataset [28] were identified using the TCGA biolinks and DESeq2 packages [29,30] using the R program, selecting those. mRNAs with an FC >1.5 and an adjusted p-value < 0.05. These DEGs were visualized using the ggplot package of R program [31].

2.6 ROC Curves Analysis

ROC curves analyses were performed based on CC and normal tissue samples from the GSE30656 dataset for *miR-19a-3p*, and the GSE67522 and GSE63514 datasets for *BDNF-AS*. These analyses were performed in GraphPad Prism v8.0 software (GraphPad Software, La Jolla, CA, USA). Area Under the Curve (AUC) values and 95% confidence intervals (CI) were calculated, and the Youden index method was used to calculate cut-off, sensitivity, specificity, and *p*-values [32].

2.7 Kaplan-Meier Curves Analysis

Overall survival (OS) was evaluated using Kaplan-Meier curves based on CC tissue samples from the TCGA dataset included in the Kaplan-Meier Plotter database [33], comparing patient outcomes when stratified based on whether *miR-19a-3p* or *BDNF-AS* expression levels fell above or below the median value. Hazard ratios (HRs) and log-rank *p*-values were calculated, and p-value < 0.05 was considered significant.

2.8 Identification of miR-19a-3p Targets

The target mRNAs of *miR-19a-3p* were identified with the miRDB [34] and TargetScan [35] databases using the default parameters. Common target mRNAs shared between these databases were identified with a Venn diagram. *miR-19a-3p* binding sites in *BDNF-AS* were identified using the Ensembl database [36].

2.9 Pathway and Biological Processes Analyses

Pathways and biological processes were analyzed using the Kyoto Encyclopedia of Genes and Genomes (KEGG) 2021 Human, Molecular Signatures Database (MSigDB) Hallmark 2020 and GO Biological Process 2021 libraries in the Enrichr database [37–40]. Log_2-transformed *p*-values were calculated for each term, with p-value $<$ 0.05 being considered significant. The Gene Set Analysis (GSEA) was done with R software. The Normalized Enrichment Score (NES) was calculated, and a p-value < 0.05 was considered as statistically significant.

2.10 Correlation Analyses

The correlation between *miR-19a-3p* and *BDNF-AS* expression in CC tissue samples in the ENCORI/StarBase (Encyclopedia of RNA interactomes) v2.0 database [41] was analyzed. The expression of *miR-19a-3p* was transformed into the Log_2 (RPM+0.01) format, while *BDNF-AS* expression was transformed into the Log_2 (FPKM+0.01) format. Correlation coefficient (R) values were calculated, and p-value < 0.05 was considered significant.

Genes correlated with *BDNF-AS* expression were identified in CC tissue samples from the TCGA dataset using the cBioportal database [42]. Genes with a Spearman's Correlation >0.30 or <-0.30, and q-value < 0.001 were selected.

Table 1. DEmiRNAs identified in CC from the GSE86100 dataset using GEO2R software.

ID	miRNA	*p*-value	FC
A_25_P00012052	*hsa-miR-196a-5p*	0.00000183	6.6
A_25_P00012078	*hsa-miR-7-5p*	0.0000000285	6.32
A_25_P00011994	*hsa-miR-18a-5p*	0.00000116	5.25
A_25_P00015381	*hsa-miR-205-3p*	0.00034	5.01
A_25_P00012034	*hsa-miR-96-5p*	0.00053	4.95
A_25_P00016153	*hsa-miR-3653*	0.00016	4.92
A_25_P00014257	*hsa-miR-590-5p*	0.0000378	4.01
A_25_P00010997	***hsa-miR-19a-3p***	**0.000229**	**3.53**
A_25_P00010954	*hsa-miR-363-3p*	0.000248	3.47
A_25_P00010614	*hsa-miR-20b-5p*	0.00000182	2.6
A_25_P00010547	*hsa-miR-141-3p*	0.000659	2.58
A_25_P00010433	*hsa-miR-106b-5p*	0.0000357	2.4
A_25_P00010975	*hsa-miR-21-5p*	0.0000574	2.27
A_25_P00010610	*hsa-miR-93-5p*	0.00000739	2.14
A_25_P00014817	*hsa-miR-15a-5p*	0.000012	2.12
A_25_P00010584	*hsa-miR-154-5p*	0.000594	–4.29
A_25_P00014342	*hsa-miR-654-3p*	0.000729	–4.32
A_25_P00015540	*hsa-miR-4253*	0.000839	–4.64
A_25_P00017457	*hsa-miR-1185-2-3p*	0.000223	–4.99
A_25_P00016710	*hsa-miR-4655-3p*	0.000202	–5.09
A_25_P00016741	*hsa-miR-4695-5p*	0.0000251	–5.39
A_25_P00015004	*hsa-miR-1226-5p*	0.00000000299	–5.71
A_25_P00015538	*hsa-miR-3137*	0.000000000464	–5.96
A_25_P00015649	*hsa-miR-3188*	0.0000152	–6.21

miRNAs in bold were selected for further analysis. FC values represent log_2-transformed fold changes.

2.11 Protein-Protein Interaction Network Construction

A protein-protein interaction (PPI) network was constructed using the Search Tool for the Retrieval of Interacting Genes/Proteins (STRING) v11.5 database [43], with the following parameters: (1) minimum required interaction score set to the highest confidence (0.900); (2) Active interaction sources: Experiments, Gene Fusion, and Co-expression; and (3) Hide disconnected nodes in the network: ON. A PPI enrichment p-value < 0.05 was considered statistically significant.

3. Results

3.1 miR-19a-3p is Upregulated in CC

To identify DEmiRNAs in CC, we analyzed the expression of miRNAs in CC tumor samples and normal tissue samples (n = 6 each) using the GSE86100 dataset with the GEO2R tool. Uniform manifold approximation and projection (UMAP) dimensionality revealed a clear separation between these tissue types, confirming that both groups were clearly distinguished (Fig. 1A). A total of 24 DEmiRNAs were identified between CC and control samples, of which 9 were downregulated, and 15 were upregulated in CC tissue samples (Table 1 and Fig. 1B).

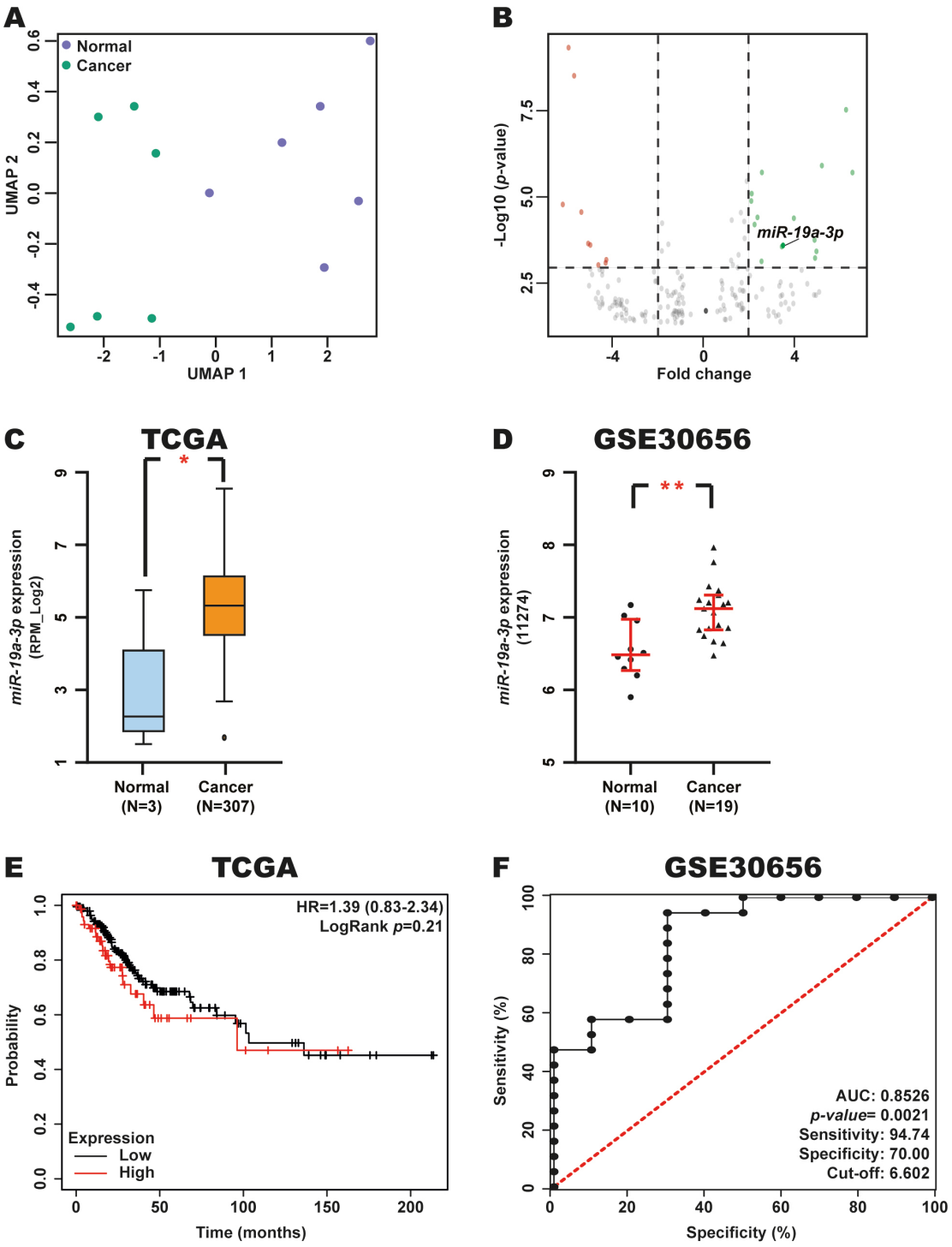

Fig. 1. Expression, diagnostic and prognostic value of *miR-19a-3p* in CC. (A) UMAP analysis of 6 CC and 6 normal tissue samples from the GSE86100 dataset. (B) Volcano plot of DEmiRNAs from the GSE86100 dataset. (C,D) Validation of *miR-19a-3p* expression in CC and normal tissue samples from the TCGA and GSE30656 datasets using the miR-TV and GEO databases. (E) Prognostic value of *miR-19a-3p* expression in patients with CC from the TCGA dataset through a Kaplan-Meier curve using the Kaplan-Meier Plotter database. Red line: high *miR-19a-3p* expression; Black line: low *miR-19a-3p* expression. (F) Diagnostic value of *miR-19a-3p* expression in CC and normal tissue samples from the GSE30656 dataset using a ROC curve in GraphPad Prism. **p*-value < 0.05; ***p*-value < 0.01. UMAP, uniform manifold approximation and projection; TCGA, The Cancer Genome Atlas; RPM, Reads Per Million; GEO, Gene Expression Omnibus; ROC, receiver operating characteristic; AUC, Area Under the Curve.

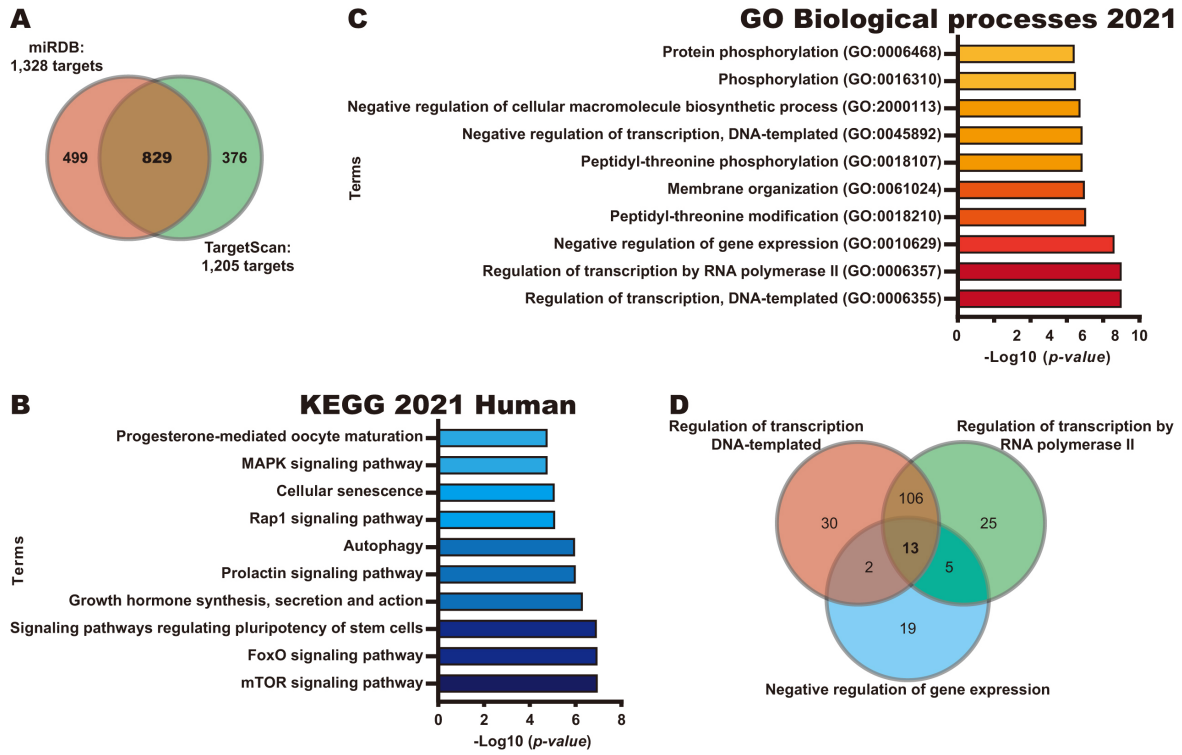

Fig. 2. Identification of potential pathways regulated by *miR-19a-3p*. (A) Identification of potential targets of *miR-19a-3p* using miRDB and TargetScan databases. (B) Pathways analysis of 829 potential targets of *miR-19a-3p* using KEGG Human 2021 library in Enrichr database. (C) BP analysis of 829 potential targets of *miR-19a-3p* using GO Biological Processes 2021 library in Enrichr database. (D) Identification of genes in common in the top three BP through a Venn diagram.

While certain miRNAs identified among these DEmiRNAs (Table 1) have previously been characterized in CC, including *miR-21-5p* [44,45] and *miR-154-5p* [46,47], others remain poorly characterized in this cancer type. Given the relatively limited research on *miR-19a-3p* in CC to date, it was chosen as a target for further analysis.

To validate changes in *miR-19a-3p* expression in CC, we analyzed the levels of this miRNA in CC and normal tissue samples from the TCGA and GSE30656 datasets using the miR-TV and GEO databases. We observed elevated *miR-19a-3p* expression in CC in these two independent datasets (Fig. 1C,D), supporting our initial findings.

To determine the potential prognostic and diagnostic relevance of *miR-19a-3p* in CC, we evaluated patient OS based on Kaplan-Meier analysis and AUC values for ROC curves when stratifying patients from the TCGA and GSE30656 datasets according to *miR-19a-3p* expression levels using the KM-Plotter database and GraphPad Prism, respectively. This analysis revealed that *miR-19a-3p* expression is not associated with OS in patients with CC (Fig. 1E). However, we found a good AUC (0.8526, p-value = 0.0021) was observed, with excellent sensitivity and specificity of 94.74% and 70.00%, respectively (Fig. 1F), for a cut-off value of 6.602.

These results suggest that *miR-19a-3p* expression is elevated in CC and that this miRNA may serve as a potential diagnostic biomarker in this type of cancer, supporting its biological and clinical relevance in this malignancy.

3.2 Identification of Potential Pathways Regulated by miR-19a-3p

To explore the potential role of *miR-19a-3p* in CC, we next identified potential targets of this miRNA using miRDB and TargetScan databases, identifying 829 common targets in both databases (Fig. 2A). Next, pathway and biological process analyses were performed for these 829 potential targets using the KEGG 2021 Human and GO Biological processes libraries from the Enrichr database. As shown in Fig. 2B, KEGG analysis revealed that the potential targets of *miR-19a-3p* participate in key pathways to CC, such as the mTOR signaling pathway, Forkhead Box O (FoxO) signaling pathway, and signaling pathways regulating pluripotency of stem cells. Interestingly, the identified biological processes were found to be involved in transcriptional regulation and protein phosphorylation, including the Regulation of transcription, DNA-template, Regulation of transcription by RNA polymerase II, and Negative regulation of gene expression processes (Fig. 2C). A Venn diagram analysis identified 13 targets of *miR-19a-3p* involved in the top 3 biological processes (Fig. 2D), including four transcription factors (ESR1, YY1, FOXP1 and REST).

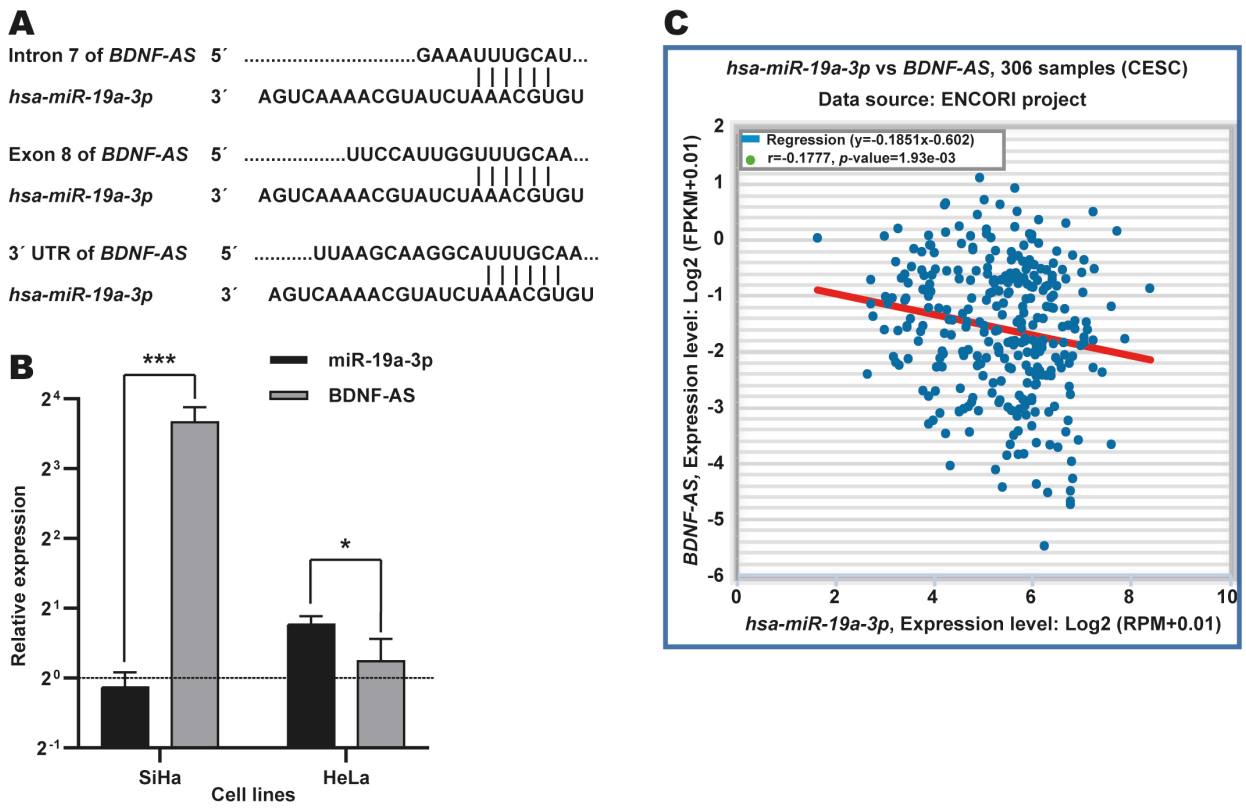

Fig. 3. Identification of *BDNF-AS* as target potential of *miR-19a-3p* in CC. (A) Identification of binding sites for *miR-19a-3p* in intron, exon and 3′ UTR regions in *BDNF-AS* using Ensembl database. (B) Expression analysis of *miR-19a-3p* in CC cell lines through RT-qPCR assays. Expression levels of *miR-19a-3p* and *BDNF-AS* were determined in HeLa and SiHa cells and they are relative to C-33A cells (dotted black line). **p*-value < 0.05; ****p*-value < 0.001. (C) Correlation analysis between *miR-19a-3p* and *BDNF-AS* expression in CC tissue samples from the TCGA dataset through ENCORI database.

Together, our results suggest that *miR-19a-3p* overexpression may inhibit the expression of its target mRNAs, affecting key pathways and processes to promote CC progression.

3.3 Identification of BDNF-AS as a Potential Target of miR-19a-3p in CC

Previous studies have reported that *miR-19a-3p* interacts with certain lncRNAs, such as *XIST* [48], *LINC00094* [49], and *KCNQ1OT1* [50]. Low levels of *BDNF-AS* expression in CC have also been reported, as has the tumor suppressor function of this lncRNA in this cancer type [51]. However, it remains unknown as to whether *miR-19a-3p* regulates *BDNF-AS* expression in CC. We therefore focused on this potential regulatory axis in CC.

To explore whether *miR-19a-3p* is involved in *BDNF-AS* regulation in CC, we searched potential binding sites for this miRNA in *BDNF-AS* using the Ensembl database. In total, three potential binding sites for this miRNA were located in *intron 7*, *exon 8*, and the *3′ UTR* (Fig. 3A) of *BDNF-AS*. In addition, RT-qPCR revealed an inverse association between the expression patterns of these two ncRNAs in SiHa and HeLa CC cells (Fig. 3B). Moreover, we observed a negative correlation between *miR-19a-3p* and *BDNF-AS* expressions in CC tissue samples from the TCGA dataset using the ENCORI database ($r = -0.1777$, p-value $= 1.93 \times 10^{-3}$) (Fig. 3C).

These results suggest that *miR-19a-3p* may regulate the expression of *BDNF-AS* in CC, which could be due to their potentially direct interaction.

3.4 BDNF-AS Expression Decreases in CC

To establish the expression of *BDNF-AS* in CC, we analyzed CC and normal tissue samples from the TCGA, GSE67522, and GSE63514 datasets using the OncoDB and GEO databases. The results revealed that *BDNF-AS* expression is decreased in CC tissue samples (Fig. 4A–C).

To investigate the diagnostic value of *BDNF-AS* expression in CC, a ROC curve analysis was performed based on the expression of this lncRNA in CC and normal samples from the GSE67522 and GSE63514 datasets using GraphPad Prism. The results revealed an AUC of 0.7170 (p-value: 0.0162) and 0.6920 (p-value: 0.0179), with sensitivities of 65.00% and 60.71%, respectively, and corresponding specificities of 68.18% and 66.67% (cutoff: 4.931 and 1.881), respectively (Fig. 4D,E). In addition, the prognos-

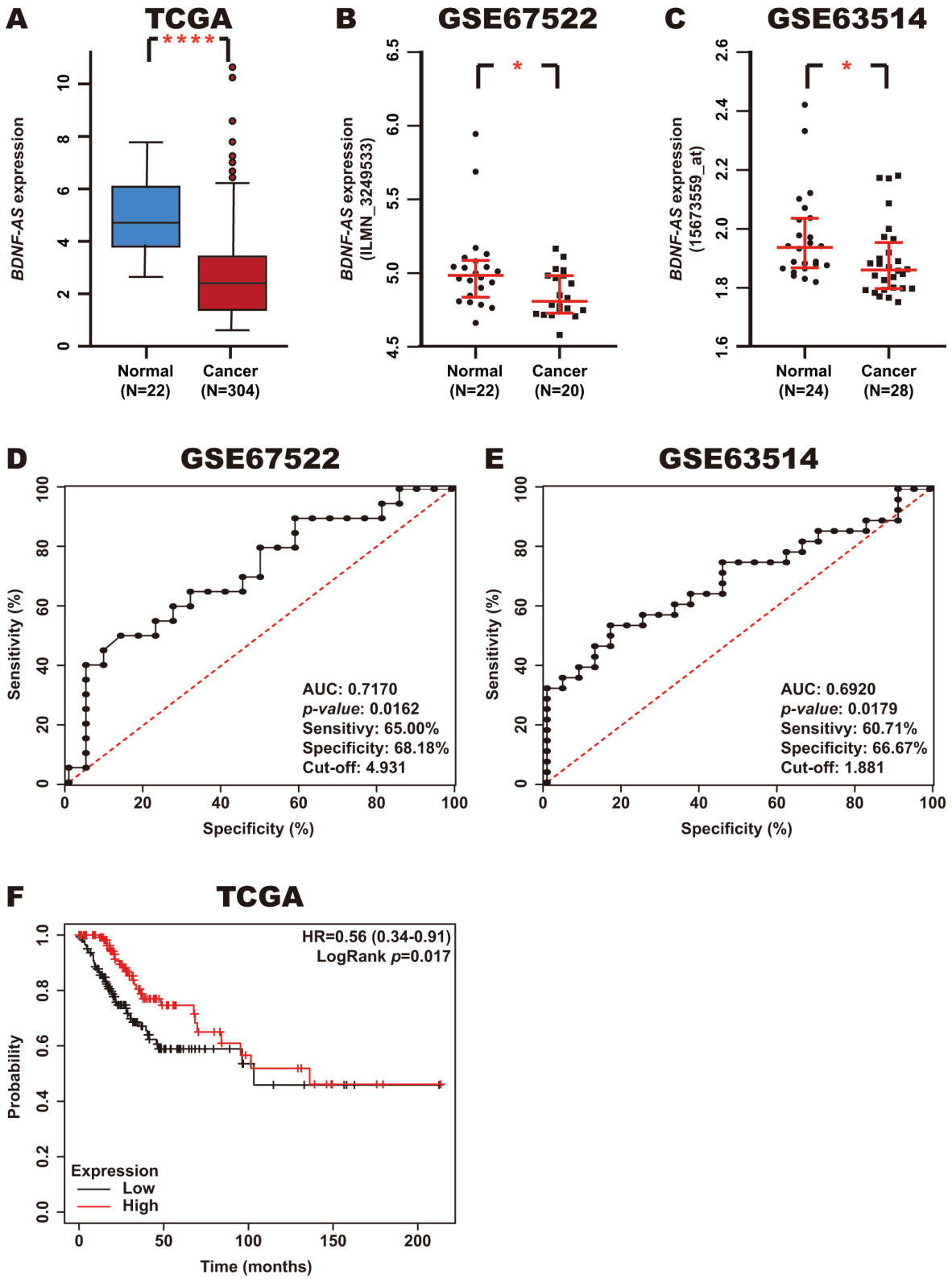

Fig. 4. Expression, diagnostic value, and prognostic value of *BDNF-AS* in CC. (A–C) *BDNF-AS* expression in CC and normal tissue samples from the TCGA, GSE67522, and GSE63514 datasets was assessed using the OncoDB and GEO databases. (D,E) The diagnostic value of *BDNF-AS* expression in CC and normal tissue samples from the GSE67522 and GSE63514 datasets was assessed using ROC curves in GraphPad Prism. (F) The prognostic value of *BDNF-AS* expression in CC tissue samples from the TCGA dataset was assessed using a Kaplan-Meier curve using the Kaplan-Meier Plotter database. Red line: high *BDNF-AS* expression; Black line: low *BDNF-AS* expression. **p*-value < 0.05; *****p*-value < 0.0001.

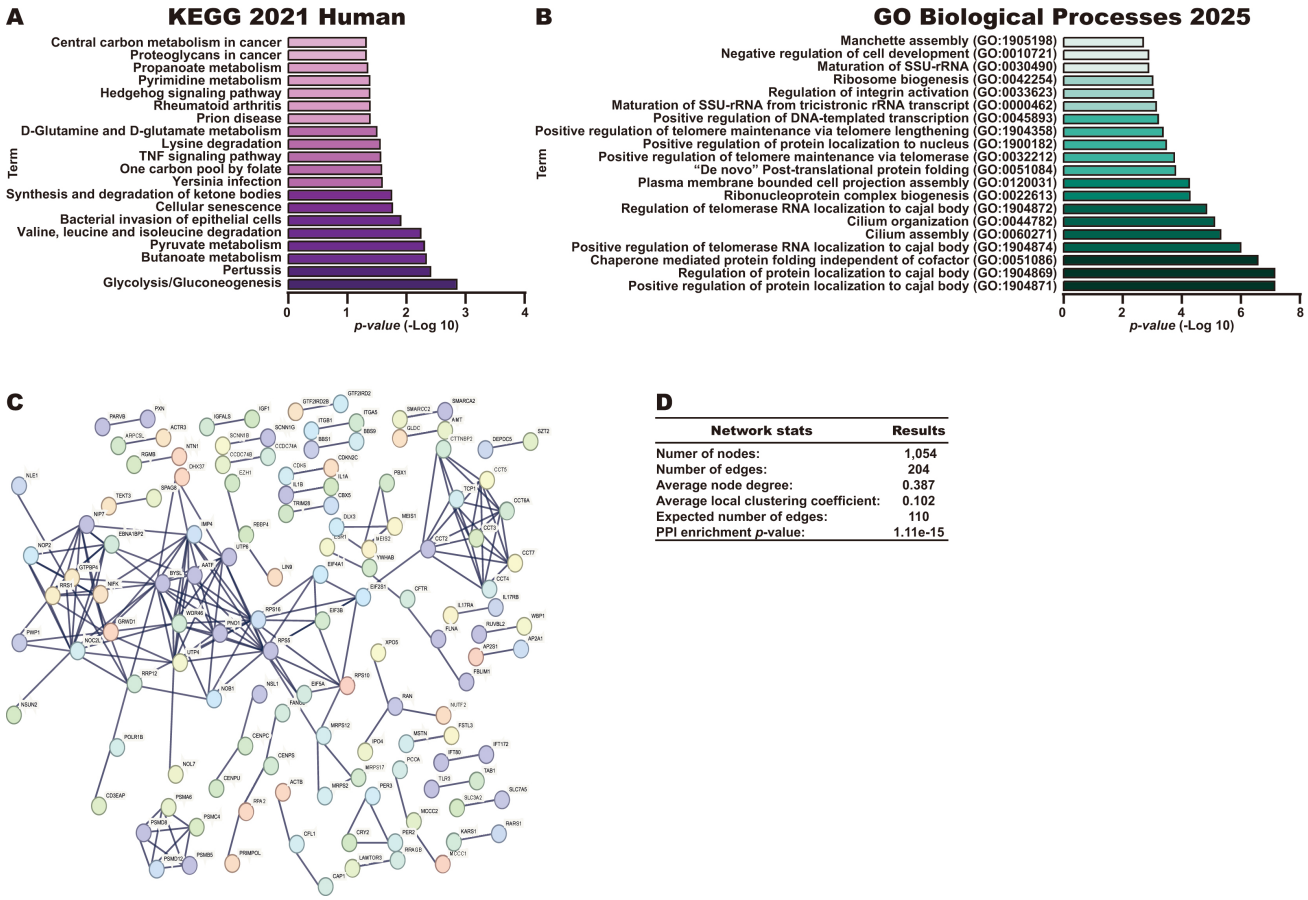

Fig. 5. Pathways and biological processes of genes that correlate with *BDNF-AS* in CC. (A) Pathways associated with the 1132 genes that were negatively or positively correlated with *BDNF-AS* expression in CC tissue samples, as assessed using the KEGG 2021 Human library in the Enrichr database. (B) The top biological process terms associated with the 1132 genes that were negatively or positively correlated with *BDNF-AS* expression, as assessed using the Biological Process 2021 library in the Enrichr database. (C,D) Construction and analysis of a PPI network incorporating the 1132 genes correlated with *BDNF-AS* expression in CC tissue samples.

tic value of *BDNF-AS* expression in CC was analyzed using a Kaplan-Meier curve in CC tissue samples from the TCGA dataset using the KM-Plotter database. Notably, low *BDNF-AS* expression was found to be associated with poor OS (Fig. 4F).

These results suggest that *BDNF-AS* expression is decreased in CC and may serve as a potential diagnostic and prognostic biomarker.

3.5 Identification of Potential Pathways Regulated by BDNF-AS in CC

To identify the potential pathways regulated by *BDNF-AS* in CC, we first identified the genes correlated with *BDNF-AS* expression in CC tissue samples from the TCGA dataset using the cBioportal database. *BDNF-AS* expression was positively correlated with the expression of 826 genes (**Supplementary Table 1**), while it was negatively correlated with the expression of 306 genes (**Supplementary Table 2**). These 1132 genes were further analyzed using the KEGG 2021 Human library in the Enrichr database. Interestingly this approach identified key pathways in CC, such as the Glycolysis/Gluconeogenesis, Cellular senescence, Tumor Necrosis Factor (TNF) signaling, Hedgehog signaling, Proteoglycans in cancer, and Central carbon metabolism in cancer pathways (Fig. 5A). In addition, biological process analysis revealed that *BDNF-AS* may be involved in processes including the following: Positive regulation of protein localization to cajal body, Ribonucleoprotein complex biogenesis, "*De novo*" Post-translational protein folding and Ribosome biogenesis (Fig. 5B). Finally, the 1132 genes were used to construct a PPI network (Fig. 5C) with 1054 nodes, 204 edges, an average node degree of 0.387, an average local clustering coefficient of 0.102, an expected number of edges of 110, and a PPI enrichment *p*-value of 1.11×10^{-15} (Fig. 5D).

In addition, we identified DEGs when comparing the top 30 CC patients with the lowest levels of *BDNF-AS* expression and the top 30 patients with the highest levels of *BDNF-AS* expression (Fig. 6A). For this comparison (low vs high *BDNF-AS* expression), 1796 DEGs were identified, including 1125 upregulated genes and 671 downregulated genes (Fig. 6B). GSEA analysis revealed that these

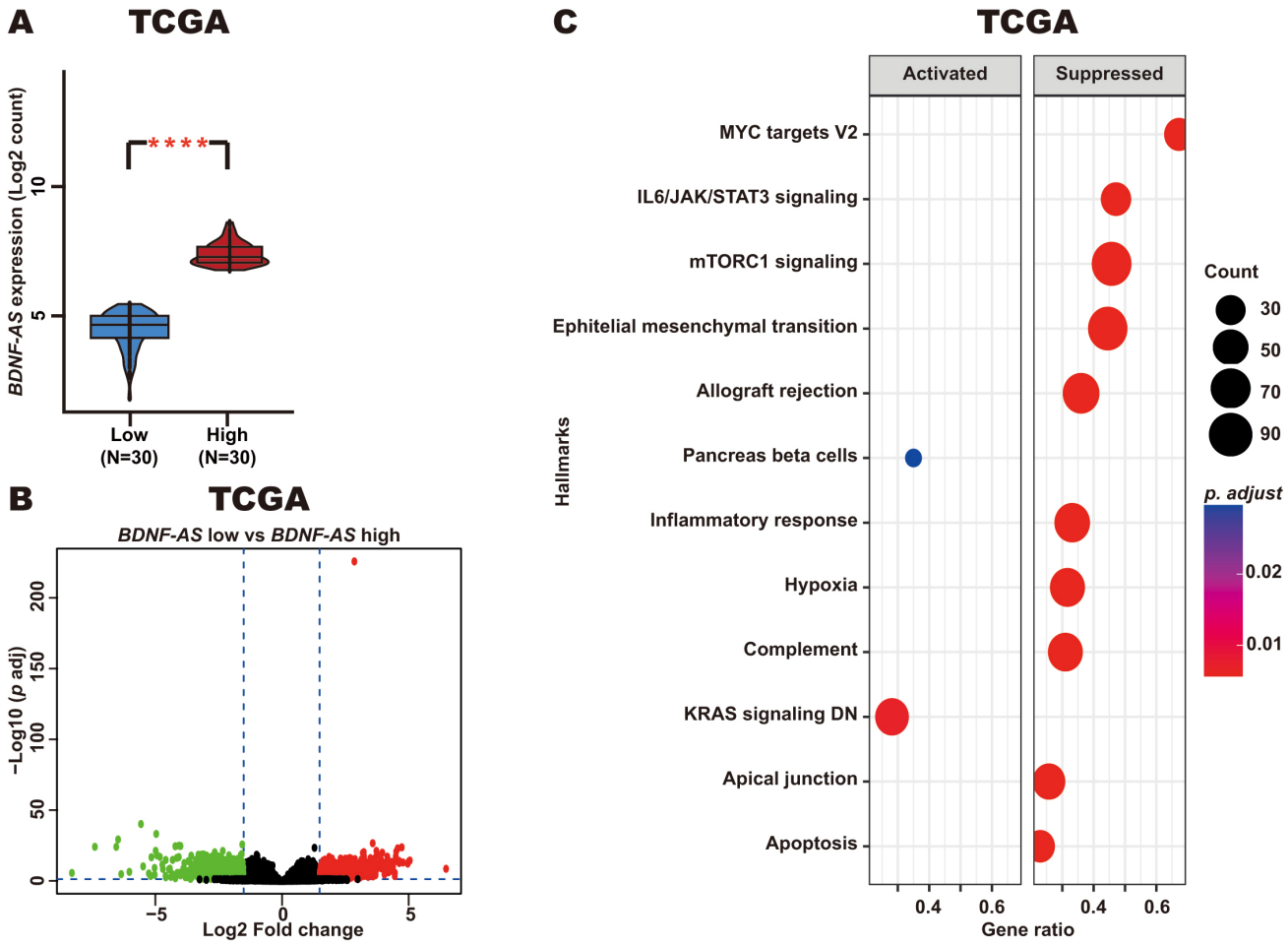

Fig. 6. Enriched pathways in CC patients with high *BDNF-AS* expression. (A) *BDNF-AS* expression in CC patients with high *BDNF-AS* expression (top 30) and low *BDNF-AS* expression (top 30) from the TCGA dataset. (B) DEGs were identified when comparing those CC patients with low and high levels of *BDNF-AS* expression from the TCGA dataset. (C) Enriched pathways derived from GSEA analysis of the identified DEGs. ****p-value < 0.0001.

DEGs were associated with key CC-related pathways, such as the apoptosis, mTORC1 signaling, and IL6/JAK/STAT3 signaling pathways. In patients with CC and high *BDNF-AS* expression, these pathways were found to be suppressed as compared with CC patients and exhibiting low levels of *BDNF-AS* expression (Fig. 6C).

These results suggest that *BDNF-AS* may be involved in the negative regulation of genes involved in key pathways related to CC pathogenesis.

4. Discussion

CC ranks as one of the top cancers among women in terms of global incidence and mortality [1]. Several studies have reported that alterations at the epigenetic level, including miRNAs, play a key role in cervical carcinogenesis, progression, and metastasis [5]. miRNAs are small molecules that regulate the expression of their target mRNAs at the post-transcriptional level, thereby affecting cellular processes, such as migration, invasion, proliferation, and apoptosis [52]. In addition, several studies have suggested that some miRNAs offer potential utility as diagnostic, prognostic, and therapeutic biomarkers in CC, including *miR-361-5p* [52,53]. There is thus value in identifying and characterizing key miRNAs in CC.

In this study, we determined that *miR-19a-3p* expression was elevated in CC in three independent RNA-seq and microarray datasets, in line with previously published RT-qPCR evidence [17], supporting our findings. Further mechanistic studies are warranted to clarify how its overexpression arises in CC, potentially through the actions of oncogenic transcription factors, copy number increases, aberrant methylation, or ncRNAs.

Analyses of CC patients OS revealed no association between high *miR-19a-3p* expression and poor patient survival. Interestingly, ROC curve analysis indicated that *miR-19a-3p* expression may offer utility as a diagnostic biomarker, although it will be crucial to validate these results in larger cohorts. Its expression can also be analyzed in serum or plasma samples to evaluate its potential use as a non-invasive biomarker. The observed differences between

the prognostic and diagnostic value of *miR-19a-3p* expression in CC in this study may be explained in part by the functional role of this miRNA in CC. For example, its diagnostic value depends on the relative levels of *miR-19a-3p* expression in CC and normal tissue samples, in line with a role in carcinogenesis, while its prognostic value solely depends on *miR-19a-3p* expression in patients with CC, in line with the participation of this miRNA disease progression, development, metastasis, and treatment response.

Previous studies have reported that *miR-19a-3p* plays a central role in CC pathogenesis as an oncomiR [17]. Recently, it has been reported that RBPMS-AS1 overexpression decreases proliferation and epithelial–mesenchymal transition activity via *miR-19a-3p*/PLCL1 axis in C-33A and HeLa CC cells [17]. In the present study, we identified several mRNA targets of *miR-19a-3p* that participate in previously reported signaling pathways, including the mTOR pathway [54], supporting our results. We also identified other pathways potentially regulated by *miR-19a-3p*, such as the FoxO signaling pathway, signaling pathways regulating the pluripotency of stem cells, and the mitogen-activated protein kinase (MAPK) signaling pathway. The FoxO signaling pathway is regulated by FoxO transcription factors, which include growth factors and stress responsive transcription factors, like FoxO1, FoxO3, FoxO4, and FoxO6. This signaling pathway regulates processes, including oxidative stress and oxidation-triggered apoptosis, and cell cycle arrest, exerting tumor suppressor activity in cancer [55]. Stem cell populations have recently been shown to function as key drivers of the initiation and progression of diseases, in addition to contributing to therapy resistance, as in prostate cancer [56]. The MAPK signaling pathway is also a major target of drug resistance in cancer [57]. Several studies have reported that these pathways are central to CC [55,58,59], underscoring the potential that *miR-19a-3p* expression may represent a therapeutic target in this type of cancer.

Biological process analysis revealed that targets of *miR-19a-3p* are involved in activities linked to transcription factor-mediated regulation of mRNA transcription. Consistently, one study reported ESR1 downregulation in CC [60,61], while another reported that REST expression decreases in high-grade squamous intraepithelial lesions and CC [62]. Our results suggest the potential existence of *miR-19a-3p*/ESR1 and *miR-19a-3p*/REST regulatory axes in CC, although this remains to be formally demonstrated.

Certain miRNAs can act as molecular sponges, thereby downregulating the expression of their mRNA targets in several human diseases, including cancer [63, 64]. *miR-19a-3p* can also be sequestered by the lncRNA RBPMS-AS1 through a ceRNA-like mechanism, inhibiting cell proliferation, growth, and EMT induction in C-33A and HeLa CC cells [17]. This molecular sponge-like activity is thus vital to the regulation of *miR-19a-3p* expression, in turn affecting the expression of its target mRNAs. In our study, the lncRNA *BDNF-AS* was identified as a potential direct target of *miR-19a-3p*. Consistently, we found that *BDNF-AS* expression was decreased in CC and negatively correlated with *miR-19a-3p* expression in CC cell lines and patient samples. These data suggest a potential *miR-19a-3p*/*BDNF-AS* axis in CC. However, these results will require experimental validation through *miR-19a-3p* knockdown, *miR-19a-3p* overexpression, and luciferase reporter assays in CC cell lines to formally test this hypothesis.

BDNF-AS acts as a tumor suppressor lncRNA in several types of cancers [65,66]. For example, one study reported that this lncRNA is downregulated in CC tissue samples and CC cell lines. In addition, *BDNF-AS* overexpression has been shown to limit the proliferation and migration of SiHa and DoTc2-4510 CC cell lines, in addition to suppressing tumor growth, while BDNF expression rescues the effects of *BDNF-AS* in these CC cell lines, suggesting that *BDNF-AS* acts as a tumor suppressor lncRNA in CC [51]. Consistently, we detected low levels of *BDNF-AS* expression in CC tissue samples from three independent RNA-seq and microarray datasets.

In addition, ROC curve analysis suggested that *BDNF-AS* expression may offer value as a diagnostic and prognostic biomarker in patients with CC, although independent cohort validation will be important. The potential value of *BDNF-AS* expression as a diagnostic and prognostic biomarker in CC patient blood samples will be of particular interest, given that this is a non-invasive analytical approach.

Moreover, KEGG and biological process analyses of genes correlated with *BDNF-AS* expression in CC revealed several important signaling pathways involved in this cancer type, including the Glycolysis/Gluconeogenesis, Cellular senescence, TNF signaling, Hedgehog signaling, Proteoglycans in cancer, and Central carbon metabolism in cancer pathways, as well as relevant biological processes. Several studies have emphasized the oncogenic role of these pathways in CC [67–71]. For example, the Hedgehog signaling pathway is vital to growth, invasion, metastasis, recurrence, drug resistance, and radioresistance in advanced CC [69]. Our results thus offer novel evidence that *BDNF-AS* reexpression may inhibit proliferation, migration and invasion through the suppresion of these pathways in CC. Future research will be necessary to test this hypothesis through functional assays in the context of *BDNF-AS* overexpression in CC cell lines. Strikingly, when we classified CC patients according to *BDNF-AS* expression and identified DEGs between samples with low and high levels of *BDNF-AS* expression, subsequent pathway analysis suggested that CC patients with high *BDNF-AS* levels exhibit the suppression of mTORC1 signaling and IL6/JAK/STAT3 signaling. Consistently, these pathways have been shown to be central to the promotion of CC development. For example, JAK/STAT3 signaling promotes CC tumor progression and metastatic development [72]. These findings are

of particular clinical relevance given that they offer an opportunity for CC patient treatment with different therapeutic approaches based on the level of *BDNF-AS* expression, potentially impacting the prognosis of the disease.

In this study, we identified a potential *miR-19a-3p*/*BDNF-AS* regulatory axis, which, if validated, could have relevant biological and clinical implications as evidenced by the results of our pathway and process analyses. Together, our results enrich our current understanding of CC biology.

5. Limitations

Our present findings are robust, as they were obtained using comprehensive databases and exhibited substantial consistency across datasets. However, all our results remain to be experimentally validated *in vitro* and *in vivo*. For example, the pathological relevance of the *miR-19a-3p*/*BDNF-AS* potential axis remains to be validated to confirm direct regulatory activity using luciferase reporter assays. Future studies are thus necessary to confirm our bioinformatic results.

6. Conclusions

In conclusion, our bioinformatic results suggest that *miR-19a-3p* may act as an oncomiR in CC. Moreover, our data suggest that this miRNA may regulate *BDNF-AS* expression in this type of cancer. However, this putative *miR-19a-3p*/*BDNF-AS* regulatory axis requires further validation. Ultimately, our findings indicate that the expression of these ncRNAs may offer potential diagnostic and prognostic utility as biomarkers in patients with CC, pending validation in larger independent clinical cohorts.

Abbreviations

CC, Cervical Cancer; miRNAs, microRNAs; lncRNA, Long non-coding RNAs; GLOBOCAN, Global Cancer Observatory: CANCER TODAY; *BDNF-AS*, Brain Derived Neurotrophic Factor-Antisense; HLA, Human Leukocyte Antigen; TCGA, The Cancer Genome Atlas; GEO, Gene Expression Omnibus; DEGs, Differentially Expressed Genes; IL6, Interleukin 6; STAT3, Signal Transducer and Activator of Transcription 3; JAK, Janus Kinase; AUC, Area Under the Curve; ROC, Receiver Operating Characteristic; TNF, Tumor Necrosis Factor; BP, Biological Processes; KEGG, Kyoto Encyclopedia of Genes and Genomes; circHIAT1, circular RNA Hippocampus Abundant Transcript 1; REST, RE1 Silencing Transcription Factor; ESR1, Estrogen Receptor 1; HPV, Human Papillomavirus; CI, Confidence Interval; mTORC1, Mechanistic Target Of Rapamycin Kinase 1; RNA-seq, RNA-sequencing; RBPMS-AS1, (RNA Binding Protein, MRNA Processing Factor)-Antisense 1; RT-qPCR, Real Time-quantitative Polymerase Chain Reaction; MAPK, Mitogen-Activated Protein Kinase; AKT, AKT Serine/Threonine Kinase; PLCL1, Phospholipase C Like 1 (Inactive); FoxO, Forkhead Box O; HR, Hazard Ratio; FPKM, Fragments Per Kilobase of exon per Million mapped reads; STRING, Search Tool for the Retrieval of Interacting Genes/Proteins; PPI, Protein-Protein Interaction; miRDB, miRNAs Data Base; ENCORI/starBase, Encyclopedia of RNA Interactomes; MSigDB, Molecular Signatures Database; GAPDH, Glyceraldehyde-3-Phosphate Dehydrogenase; FC, Fold Change.

Availability of Data and Materials

The data presented in this study are available in miRTV, OncoDB and GEO databases at https://mirtv.ibms.sinica.edu.tw/, https://oncodb.org/, and https://www.ncbi.nlm.nih.gov/geo/ with the reference number [19,20] and [21–27], respectively. The datasets used and analyzed during the current study are available from the corresponding author on reasonable request.

Author Contributions

HJW and EGSB: conceptualization. RAA, JOO, AAI, AFR: methodology. FITR, RDM and FDBA: validation. RAA, AAI and GECV: formal analysis. RAA and JAM: investigation. RDM, GECV and RAA: data curation. RAA, AAI and HJW: writing—original draft preparation. EGSB: writing—review and editing. HJW and EGSB: supervision. All authors contributed to editorial changes in the manuscript. All authors read and approved the final manuscript. All authors have participated sufficiently in the work and agreed to be accountable for all aspects of the work.

Ethics Approval and Consent to Participate

Not applicable.

Acknowledgment

Not applicable.

Funding

This research received no external funding.

Conflicts of Interest

The authors declare no conflicts of interest.

Supplementary Material

Supplementary material associated with this article can be found, in the online version, at https://doi.org/10.31083/FBL51227.

References

[1] Bray F, Laversanne M, Sung H, Ferlay J, Siegel RL, Soerjomataram I, *et al*. Global cancer statistics 2022: GLOBOCAN estimates of incidence and mortality worldwide for 36 cancers

in 185 countries. CA: A Cancer Journal for Clinicians. 2024; 74: 229–263. https://doi.org/10.3322/caac.21834.

[2] Siegel RL, Giaquinto AN, Jemal A. Cancer statistics, 2024. CA: A Cancer Journal for Clinicians. 2024; 74: 12–49. https://doi.org/10.3322/caac.21820.

[3] Okunade KS. Human papillomavirus and cervical cancer. Journal of Obstetrics and Gynaecology: the Journal of the Institute of Obstetrics and Gynaecology. 2020; 40: 602–608. https://doi.org/10.1080/01443615.2019.1634030.

[4] Ramachandran D, Dörk T. Genomic Risk Factors for Cervical Cancer. Cancers. 2021; 13: 5137. https://doi.org/10.3390/cancers13205137.

[5] Liu H, Ma H, Li Y, Zhao H. Advances in epigenetic modifications and cervical cancer research. Biochimica et Biophysica Acta. Reviews on Cancer. 2023; 1878: 188894. https://doi.org/10.1016/j.bbcan.2023.188894.

[6] Nemeth K, Bayraktar R, Ferracin M, Calin GA. Non-coding RNAs in disease: from mechanisms to therapeutics. Nature Reviews. Genetics. 2024; 25: 211–232. https://doi.org/10.1038/s41576-023-00662-1.

[7] Saliminejad K, Khorram Khorshid HR, Soleymani Fard S, Ghaffari SH. An overview of microRNAs: Biology, functions, therapeutics, and analysis methods. Journal of Cellular Physiology. 2019; 234: 5451–5465. https://doi.org/10.1002/jcp.27486.

[8] Ebert MS, Sharp PA. Emerging roles for natural microRNA sponges. Current Biology: CB. 2010; 20: R858–R861. https://doi.org/10.1016/j.cub.2010.08.052.

[9] Gaiti F, Degnan BM, Tanurdžić M. Long non-coding regulatory RNAs in sponges and insights into the origin of animal multicellularity. RNA Biology. 2018; 15: 696–702. https://doi.org/10.1080/15476286.2018.1460166.

[10] Darbeheshti F, Mansoori Y, Azizi-Tabesh G, Zolfaghari F, Kadkhoda S, Rasti A, *et al*. Evaluation of Circ_0000977-Mediated Regulatory Network in Breast Cancer: A Potential Discriminative Biomarker for Triple-Negative Tumors. Biochemical Genetics. 2023; 61: 1487–1508. https://doi.org/10.1007/s10528-023-10331-x.

[11] Smolarz B, Durczyński A, Romanowicz H, Szyłło K, Hogendorf P. miRNAs in Cancer (Review of Literature). International Journal of Molecular Sciences. 2022; 23: 2805. https://doi.org/10.3390/ijms23052805.

[12] Ardekani AM, Naeini MM. The Role of MicroRNAs in Human Diseases. Avicenna Journal of Medical Biotechnology. 2010; 2: 161–179.

[13] Wei Z, Wang W, Li Q, Du L, He X. The microRNA *miR-19a-3p* suppresses cell growth, migration, and invasion in multiple myeloma via the Wnt/β-catenin pathway. Translational Cancer Research. 2021; 10: 1053–1064. https://doi.org/10.21037/tcr-20-3490.

[14] Jiang XM, Yu XN, Liu TT, Zhu HR, Shi X, Bilegsaikhan E, *et al*. microRNA-19a-3p promotes tumor metastasis and chemoresistance through the PTEN/Akt pathway in hepatocellular carcinoma. Biomedicine & Pharmacotherapy = Biomedecine & Pharmacotherapie. 2018; 105: 1147–1154. https://doi.org/10.1016/j.biopha.2018.06.097.

[15] Zhang H, Zhu J, Zhang J, Liu Y, Zhao B, Yang X, *et al*. *miR-19a-3p* promotes the growth of hepatocellular carcinoma by regulating p53/SOX4. Heliyon. 2024; 10: e36282. https://doi.org/10.1016/j.heliyon.2024.e36282.

[16] Peng T, Yang F, Sun Z, Yan J. *miR-19a-3p* Facilitates Lung Adenocarcinoma Cell Phenotypes by Inhibiting TEK. Cancer Biotherapy & Radiopharmaceuticals. 2022; 37: 589–601. https://doi.org/10.1089/cbr.2020.4456.

[17] Huang L, Shen Q, Yu K, Yang J, Li X. RBPMS-AS1 sponges *miR-19a-3p* to restrain cervical cancer cells via enhancing PLCL1-mediated pyroptosis. Biotechnology and Applied Biochemistry. 2025; 72: 340–354. https://doi.org/10.1002/bab.2667.

[18] Livak KJ, Schmittgen TD. Analysis of relative gene expression data using real-time quantitative PCR and the 2(-Delta Delta C(T)) Method. Methods (San Diego, Calif.). 2001; 25: 402–408. https://doi.org/10.1006/meth.2001.1262.

[19] Gao D, Zhang Y, Zhu M, Liu S, Wang X. miRNA Expression Profiles of HPV-Infected Patients with Cervical Cancer in the Uyghur Population in China. PloS One. 2016; 11: e0164701. https://doi.org/10.1371/journal.pone.0164701.

[20] Barrett T, Wilhite SE, Ledoux P, Evangelista C, Kim IF, Tomashevsky M, *et al*. NCBI GEO: archive for functional genomics data sets–update. Nucleic Acids Research. 2013; 41: D991–D995. https://doi.org/10.1093/nar/gks1193.

[21] Pan C-Y, Lin W-C. miR-TV: an interactive microRNA Target Viewer for microRNA and target gene expression interrogation for human cancer studies. Database: The Journal of Biological Databases and Curation. 2020; 2020: baz148. https://doi.org/10.1093/database/baz148.

[22] Tang G, Cho M, Wang X. OncoDB: an interactive online database for analysis of gene expression and viral infection in cancer. Nucleic Acids Research. 2022; 50: D1334–D1339. https://doi.org/10.1093/nar/gkab970.

[23] Wilting SM, Snijders PJF, Verlaat W, Jaspers A, van de Wiel MA, van Wieringen WN, *et al*. Altered microRNA expression associated with chromosomal changes contributes to cervical carcinogenesis. Oncogene. 2013; 32: 106–116. https://doi.org/10.1038/onc.2012.20.

[24] Saha SS, Chowdhury RR, Mondal NR, Roy S, Sengupta S. Expression signatures of HOX cluster genes in cervical cancer pathogenesis: Impact of human papillomavirus type 16 oncoprotein E7. Oncotarget. 2017; 8: 36591–36602. https://doi.org/10.18632/oncotarget.16619.

[25] Sharma S, Mandal P, Sadhukhan T, Roy Chowdhury R, Ranjan Mondal N, Chakravarty B, *et al*. Bridging Links between Long Noncoding RNA HOTAIR and HPV Oncoprotein E7 in Cervical Cancer Pathogenesis. Scientific Reports. 2015; 5: 11724. https://doi.org/10.1038/srep11724.

[26] den Boon JA, Pyeon D, Wang SS, Horswill M, Schiffman M, Sherman M, *et al*. Molecular transitions from papillomavirus infection to cervical precancer and cancer: Role of stromal estrogen receptor signaling. Proceedings of the National Academy of Sciences of the United States of America. 2015; 112: E3255–E3264. https://doi.org/10.1073/pnas.1509322112.

[27] Edgar R, Domrachev M, Lash AE. Gene Expression Omnibus: NCBI gene expression and hybridization array data repository. Nucleic Acids Research. 2002; 30: 207–210. https://doi.org/10.1093/nar/30.1.207.

[28] Cancer Genome Atlas Research Network, Weinstein JN, Collisson EA, Mills GB, Shaw KRM, Ozenberger BA, *et al*. The Cancer Genome Atlas Pan-Cancer analysis project. Nature Genetics. 2013; 45: 1113–1120. https://doi.org/10.1038/ng.2764.

[29] Colaprico A, Silva TC, Olsen C, Garofano L, Cava C, Garolini D, *et al*. TCGAbiolinks: an R/Bioconductor package for integrative analysis of TCGA data. Nucleic Acids Research. 2016; 44: e71. https://doi.org/10.1093/nar/gkv1507.

[30] Love MI, Huber W, Anders S. Moderated estimation of fold change and dispersion for RNA-seq data with DESeq2. Genome Biology. 2014; 15: 550. https://doi.org/10.1186/s13059-014-0550-8.

[31] Wickham H. ggplot2. Springer International Publishing: Cham. 2016.

[32] YOUDEN WJ. Index for rating diagnostic tests. Cancer. 1950; 3: 32–35. https://doi.org/10.1002/1097-0142(1950)3:1<32::aid-cncr2820030106>3.0.co;2-3.

[33] Nagy Á, Munkácsy G, Győrffy B. Pancancer survival analysis

of cancer hallmark genes. Scientific Reports. 2021; 11: 6047. https://doi.org/10.1038/s41598-021-84787-5.

[34] Chen Y, Wang X. miRDB: an online database for prediction of functional microRNA targets. Nucleic Acids Research. 2020; 48: D127–D131. https://doi.org/10.1093/nar/gkz757.

[35] Agarwal V, Bell GW, Nam JW, Bartel DP. Predicting effective microRNA target sites in mammalian mRNAs. eLife. 2015; 4: e05005. https://doi.org/10.7554/eLife.05005.

[36] Dyer SC, Austine-Orimoloye O, Azov AG, Barba M, Barnes I, Barrera-Enriquez VP, *et al*. Ensembl 2025. Nucleic Acids Research. 2025; 53: D948–D957. https://doi.org/10.1093/nar/gkae1071.

[37] Chen EY, Tan CM, Kou Y, Duan Q, Wang Z, Meirelles GV, *et al*. Enrichr: interactive and collaborative HTML5 gene list enrichment analysis tool. BMC Bioinformatics. 2013; 14: 128. https://doi.org/10.1186/1471-2105-14-128.

[38] Kuleshov MV, Jones MR, Rouillard AD, Fernandez NF, Duan Q, Wang Z, *et al*. Enrichr: a comprehensive gene set enrichment analysis web server 2016 update. Nucleic Acids Research. 2016; 44: W90–7. https://doi.org/10.1093/nar/gkw377.

[39] Xie Z, Bailey A, Kuleshov MV, Clarke DJB, Evangelista JE, Jenkins SL, *et al*. Gene Set Knowledge Discovery with Enrichr. Current Protocols. 2021; 1: e90. https://doi.org/10.1002/cpz1.90.

[40] Ali A, Hulipalled VR, Patil SS, Abdulkader R. DPEBic: detecting essential proteins in gene expressions using encoding and biclustering algorithm. Journal of Ambient Intelligence and Humanized Computing. 2021. https://doi.org/10.1007/s12652-021-03036-9.

[41] Li JH, Liu S, Zhou H, Qu LH, Yang JH. starBase v2.0: decoding miRNA-ceRNA, miRNA-ncRNA and protein-RNA interaction networks from large-scale CLIP-Seq data. Nucleic Acids Research. 2014; 42: D92–D97. https://doi.org/10.1093/nar/gkt1248.

[42] Cerami E, Gao J, Dogrusoz U, Gross BE, Sumer SO, Aksoy BA, *et al*. The cBio cancer genomics portal: an open platform for exploring multidimensional cancer genomics data. Cancer Discovery. 2012; 2: 401–404. https://doi.org/10.1158/2159-8290.CD-12-0095.

[43] Szklarczyk D, Franceschini A, Wyder S, Forslund K, Heller D, Huerta-Cepas J, *et al*. STRING v10: protein-protein interaction networks, integrated over the tree of life. Nucleic Acids Research. 2015; 43: D447–D452. https://doi.org/10.1093/nar/gku1003.

[44] Chen Y, Su C, Cai Y, Ke L, Huang Y. miR-21 promotes cervical cancer by regulating NTF3. Scientific Reports. 2025; 15: 2442. https://doi.org/10.1038/s41598-025-85888-1.

[45] Aguilar-Martínez SY, Campos-Viguri GE, Medina-García SE, García-Flores RJ, Deas J, Gómez-Cerón C, *et al*. MiR-21 Regulates Growth and Migration of Cervical Cancer Cells by RECK Signaling Pathway. International Journal of Molecular Sciences. 2024; 25: 4086. https://doi.org/10.3390/ijms25074086.

[46] Li Y, Wei Y, Zhang H, Bai Y, Wang X, Li Q, *et al*. MicroRNA-154-5p suppresses cervical carcinoma growth and metastasis by silencing Cullin2 *in vitro* and *in vivo*. PeerJ. 2023; 11: e15641. https://doi.org/10.7717/peerj.15641.

[47] Zhao W, Liu Y, Zhang L, Ding L, Li Y, Zhang H, *et al*. MicroRNA-154-5p regulates the HPV16 E7-pRb pathway in Cervical Carcinogenesis by targeting CUL2. Journal of Cancer. 2020; 11: 5379–5389. https://doi.org/10.7150/jca.45871.

[48] Chen S, Li Y, Zhi S, Ding Z, Huang Y, Wang W, *et al*. lncRNA Xist Regulates Osteoblast Differentiation by Sponging *miR-19a-3p* in Aging-induced Osteoporosis. Aging and Disease. 2020; 11: 1058–1068. https://doi.org/10.14336/AD.2019.0724.

[49] Xiang Y, Liu H, Hu H, Li LW, Zong QB, Wu TW, *et al*. LINC00094/*miR-19a-3p*/CYP19A1 axis affects the sensitivity of ER positive breast cancer cells to Letrozole through EMT pathway. Aging. 2022; 14: 4755–4768. https://doi.org/10.18632/aging.204110.

[50] Lin H, Nie L, Lu G, Wu H, Xu T. Long non-coding RNA KCNQ10T1/*miR-19a-3p*/SMAD5 axis promotes osteogenic differentiation of mouse bone mesenchymal stem cells. Journal of Orthopaedic Surgery and Research. 2023; 18: 929. https://doi.org/10.1186/s13018-023-04425-w.

[51] Zhang H, Liu C, Yan T, Wang J, Liang W. Long noncoding RNA *BDNF-AS* is downregulated in cervical cancer and has anti-cancer functions by negatively associating with BDNF. Archives of Biochemistry and Biophysics. 2018; 646: 113–119. https://doi.org/10.1016/j.abb.2018.03.023.

[52] Causin RL, Freitas AJAD, Hidalgo Filho CMT, Reis RD, Reis RM, Marques MMC. A Systematic Review of MicroRNAs Involved in Cervical Cancer Progression. Cells. 2021; 10: 668. https://doi.org/10.3390/cells10030668.

[53] Gao F, Feng J, Yao H, Li Y, Xi J, Yang J. LncRNA SBF2-AS1 promotes the progression of cervical cancer by regulating miR-361-5p/FOXM1 axis. Artificial Cells, Nanomedicine, and Biotechnology. 2019; 47: 776–782. https://doi.org/10.1080/21691401.2019.1577883.

[54] Ji J, Zheng PS. Activation of mTOR signaling pathway contributes to survival of cervical cancer cells. Gynecologic Oncology. 2010; 117: 103–108. https://doi.org/10.1016/j.ygyno.2009.12.020.

[55] Farhan M, Wang H, Gaur U, Little PJ, Xu J, Zheng W. FOXO Signaling Pathways as Therapeutic Targets in Cancer. International Journal of Biological Sciences. 2017; 13: 815–827. https://doi.org/10.7150/ijbs.20052.

[56] Zhang X, Zhang X, Bao Q, Li R, Deng X, Cao J, *et al*. Cancer stem cell plasticity in shaping drug resistance landscapes in prostate cancer. Journal of Advanced Research. 2025. https://doi.org/10.1016/j.jare.2025.09.028. (online ahead of print)

[57] Kadasah SF. Targeting the MAPK Pathway in Cancer. International Journal of Molecular Sciences. 2025; 27: 214. https://doi.org/10.3390/ijms27010214.

[58] Mendoza-Almanza G, Ortíz-Sánchez E, Rocha-Zavaleta L, Rivas-Santiago C, Esparza-Ibarra E, Olmos J. Cervical cancer stem cells and other leading factors associated with cervical cancer development. Oncology Letters. 2019; 18: 3423–3432. https://doi.org/10.3892/ol.2019.10718.

[59] Liao J, Deng S, Shi B, Wang M, Yin Y, Cao Y, *et al*. HPV16 E7 inhibits HBD2 expression by down-regulation of ASK1-p38 MAPK pathway in cervical cancer. Virology Journal. 2025; 22: 109. https://doi.org/10.1186/s12985-025-02731-9.

[60] Zhai Y, Bommer GT, Feng Y, Wiese AB, Fearon ER, Cho KR. Loss of estrogen receptor 1 enhances cervical cancer invasion. The American Journal of Pathology. 2010; 177: 884–895. https://doi.org/10.2353/ajpath.2010.091166.

[61] Ali A, Mohan J, Nadaf TAA, Ravishankar H, Deepa K. Bioinformatics-driven discovery of signaling pathways and genes influencing cervical cancer. SN Computer Science. 2024; 5: 989.

[62] Cortés-Sarabia K, Alarcón-Romero LDC, Flores-Alfaro E, Illades-Aguiar B, Vences-Velázquez A, Mendoza-Catalán MÁ, *et al*. Significant decrease of a master regulator of genes (REST/NRSF) in high-grade squamous intraepithelial lesion and cervical cancer. Biomedical Journal. 2021; 44: S171–S178. https://doi.org/10.1016/j.bj.2020.08.012.

[63] Ebert MS, Sharp PA. MicroRNA sponges: progress and possibilities. RNA (New York, N.Y.). 2010; 16: 2043–2050. https://doi.org/10.1261/rna.2414110.

[64] Huang J, Yu S, Ding L, Ma L, Chen H, Zhou H, *et al*. The Dual Role of Circular RNAs as miRNA Sponges in Breast Cancer and Colon Cancer. Biomedicines. 2021; 9: 1590. https://doi.org/10.

3390/biomedicines9111590.

[65] Zhi H, Lian J. LncRNA *BDNF-AS* suppresses colorectal cancer cell proliferation and migration by epigenetically repressing GSK-3β expression. Cell Biochemistry and Function. 2019; 37: 340–347. https://doi.org/10.1002/cbf.3403.

[66] Zhao H, Diao C, Wang X, Xie Y, Liu Y, Gao X, *et al*. LncRNA *BDNF-AS* inhibits proliferation, migration, invasion and EMT in oesophageal cancer cells by targeting miR-214. Journal of Cellular and Molecular Medicine. 2018; 22: 3729–3739. https://doi.org/10.1111/jcmm.13558.

[67] He Y, Qiu Y, Yang X, Lu G, Zhao SS. Remodeling of tumor microenvironment by cellular senescence and immunosenescence in cervical cancer. Seminars in Cancer Biology. 2025; 108: 17–32. https://doi.org/10.1016/j.semcancer.2024.11.002.

[68] Chen X, Lin L, Wu Q, Li S, Wang H, Sun Y. Tumor Necrosis Factor-α Promotes the Tumorigenesis, Lymphangiogenesis, and Lymphatic Metastasis in Cervical Cancer via Activating VEGFC-Mediated AKT and ERK Pathways. Mediators of Inflammation. 2023; 2023: 5679966. https://doi.org/10.1155/2023/5679966.

[69] Liu C, Wang R. The Roles of Hedgehog Signaling Pathway in Radioresistance of Cervical Cancer. Dose-response: a Publication of International Hormesis Society. 2019; 17: 1559325819885293. https://doi.org/10.1177/1559325819885293.

[70] Zhou Y, Zhang C, Wei H, Ding S, Li H, Hao Y. Directed evolution of proteoglycan-modifying enzymes: Functional applications in cervical cancer therapy. International Journal of Biological Macromolecules. 2025; 304: 140659. https://doi.org/10.1016/j.ijbiomac.2025.140659.

[71] Li B, Sui L. Metabolic reprogramming in cervical cancer and metabolomics perspectives. Nutrition & Metabolism. 2021; 18: 93. https://doi.org/10.1186/s12986-021-00615-7.

[72] Gutiérrez-Hoya A, Soto-Cruz I. Role of the JAK/STAT Pathway in Cervical Cancer: Its Relationship with HPV E6/E7 Oncoproteins. Cells. 2020; 9: 2297. https://doi.org/10.3390/cells9102297.